Thermal Behavior and Heat Generation Modeling of Lithium Sulfur Batteries

Stroe, Daniel-Ioan; Knap, Vaclav; Swierczynski, Maciej Jozef; Schaltz, Erik

Published in:
ECS Transactions

DOI (link to publication from Publisher):
10.1149/07711.0467ecst

Publication date:
2017

Document Version
Accepted author manuscript, peer reviewed version

Thermal Behavior and Heat Generation Modeling of Lithium Sulfur Batteries

D.-I. Stroe[a], V. Knap[a], M. Swierczynski[a], E. Schaltz[a]

[a] Department of Energy Technology, Aalborg University, Aalborg 9220, Denmark

Lithium Sulfur batteries are receiving a lot of research interest because of their intrinsic characteristics, such as very high energy density and increased safety, which make them a suitable solution for zero-emission vehicles and space application. This paper analyses the influence of the temperature on the performance parameters of a 3.4 Ah Lithium-Sulfur battery cell. Furthermore, the values of the internal resistance and entropic heat coefficient, which are necessary for the parametrization of a heat generation model, are determined experimentally.

Introduction

In the past years a lot of research has been carried out in order to develop batteries with very high energy density levels and improved safety, which could fulfill the requirements of next generation electrical vehicle and military applications. This is the case of Lithium-Sulfur (Li-S) batteries, which are characterized at present by very high theoretical specific capacity (i.e., 1675 mAh/g) and energy density (2600 Wh/kg) as well as improved safety levels (1). However, their market penetration at a large scale is prevented by their inherent polysulfide shuttle mechanism, which causes fast capacity fade and poor coulombic efficiency (2). Thus, research and development efforts are carried out in order to improve this chemistry (3).

Several aspects regarding the electrical and lifetime behavior of LiS batteries have been studied and are presented in literature. For example, in (4), the authors have analyzed the self-discharge behavior of Li-S batteries; high temperatures and increased state-of-charge (SOC) levels were found to enhance the self-discharge process. Stroe et al, have performed an in-depth electrochemical impedance spectroscopy characterization of a Li-S pouch battery cell (5); the influence on the SOC and temperature on the development of the Li-S battery cell's impedance spectra was thoroughly investigated. A Li-S battery cell electric model was developed and parametrized for various discharging conditions in (6). Furthermore, the degradation mechanisms responsible for Li-S battery cells' lifetime reduction were studied in (7).

Besides the electrical and lifetime characteristics, the thermal behavior of batteries is equally important. However, so far only few studies have focused on thermal aspects related to Li-S battery cells; furthermore, most of these studies were performed in laboratory assembled coin cells. For example, isothermal micro-calorimetry was used in (8) to measure the heat generation during discharging of a Li-S coin cell. A transient method for the simulation of Li-S cells characteristics is developed in (9).

In this work, we characterize the thermal behavior of a pre-commercial 3.4 Ah Li-S battery cell. The dependence of the cell's capacity on the temperature and current rate is investigated and the temperature evolution during cell discharging at different conditions is analyzed and quantified. Furthermore, the internal resistance, which is responsible for the cell's polarization heat, is determined at different temperatures (i.e., 10°C, 25°C, and 40°C) for the whole SOC interval. Lastly, by performing open circuit potentiometry measurements, the entropic heat coefficient of the tested Li-S battery cell was determined and its variation with the SOC is presented and analyzed. The results of all these measurements can be further used to parameterize a simple but comprehensive battery heat generation model.

Experimental Set-Up

This work was carried out using a long-life type Li-S pouch cell manufactured by OXIS Energy. The electrical parameters of the Li-S cell are presented in Table I.

TABLE I. Main electrical and thermal parameters of the Li-S battery cell.

Parameter	Value
Nominal Capacity	3.4 Ah
Nominal Voltage	2.05 V
Maximum Voltage	2.45 V
Minimum Voltage	1.5 V
Nominal Charging Current	0.34 A (1 C-rate)
Nominal Discharging Current	0.68 A (2 C-rate)
Temperature Operation Range	+5°C to +80°C

All the experiments were performed using a MACCOR 4000 series battery test station. During the experiments the Li-S pouch cell was placed inside a temperature-controlled climatic chamber, as illustrated in Figure 1. The temperature of the cell was monitored using a type-K thermocouple; furthermore, the temperature values referred in the following are the ones measured on the surface of the Li-S battery cell.

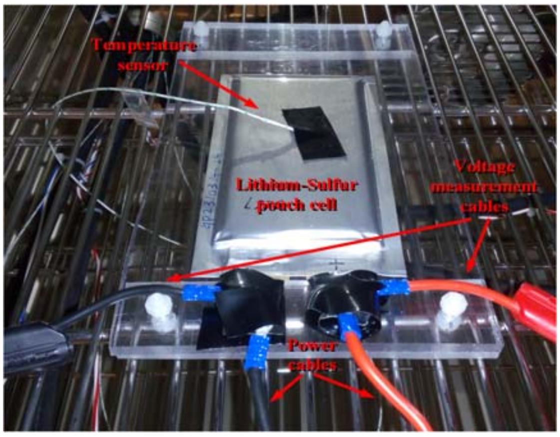

Figure 1. Li-S pouch cell placed inside the climatic chamber during the thermal characterization procedure.

Heat Generation Modeling

To build a battery thermal model, the equation for energy balance has to be considered for a given battery cooling or heating scenario. A general energy balance equation for battery systems was proposed by Bernardi et al in (10). Nevertheless, if adiabatic conditions are considered, the energy balance equation can be simplified and the accumulation of enthalpy in the battery cell will match the heat generation (11):

$$M \cdot Cp \cdot dT / dt = I^2 \cdot Ri + I \cdot T \cdot \delta Uavg / \delta T \quad [1]$$

Where, *M* represents the mass of the cell, *C*p represents the mean heat capacity a constant pressure, *T* represents the temperature, *t* represents the time, *I* represents the battery cell current, *R*i represents the internal resistance, and *U*avg represents the open circuit potential.

The battery heat generation, Pgen, is expressed as in [2]. The first term in [2], known as polarization heat, is a function of the cell's internal resistance and is composed of the Joule heating within the cell and the energy dissipated in the electrode overpotentials (11). This term is always positive meaning that the polarization heat is exothermic during both charging and discharging conditions. The second term in [2] is the reversible entropic heat and is related to the entropy change; the derivative of the potential in respect to temperature is the entropic heat coefficient (EHC), which can take either positive or negative values.

$$Pgen = I^2 \cdot Ri + I \cdot T \cdot \delta Uavg / \delta T \quad [2]$$

Thus, in order to be able to determine the heat generation of the studied Li-S battery cell, the internal resistance and the EHC have to be determined. The procedures used to determine these thermal parameters and the obtained results are presented throughout the next section.

Heat Generation Model Parametrization

In order to parameterize the heat generation model of the Li-S battery cell, the internal resistance and EHC had to be measured. Another battery performance parameter, which is temperature dependent and it was measured, is the battery capacity; furthermore, the battery capacity should be known in order to set the state-of-charge at which the internal resistance and EHC are measured. In the following, the used procedures to measure the battery capacity, internal resistance, and EHC are detailed and subsequently, the obtained laboratory results are presented.

Capacity Measurement

In order to determine the variation of the capacity of the studied Li-S battery cell with the temperature, measurements at three temperatures (i.e., 10°C, 25°C, and 40°C) were performed. Furthermore, the capacity measurements were repeated during discharge at three different C-rates, i.e., 0.2 C-rate (0.68 A), 0.5 C-rate (1.7 A), and 1 C-rate (3.4 A). Before each discharging, the Li-S battery was fully re-charged with 0.1 C-rate (0.34 A).

The procedure to measure the capacity of the Li-S battery cell was as follows:

0. Tempering of the cell for two hours at 10°C
1. Two preconditioning cycle; charging with 0.1 C-rate (0.34 A) and discharging with 0.2 C-rate (0.68 A);
2. Capacity measurement at 0.2 C-rate; charging with 0.1 C-rate (0.34 A) and discharging with 0.2 C-rate (0.68 A);
3. Capacity measurement at 0.5 C-rate; charging with 0.1 C-rate (0.34 A) and discharging with 0.5 C-rate (1.7 A);
4. One preconditioning cycle; charging with 0.1 C-rate (0.34 A) and discharging with 0.2 C-rate (0.68 A);
5. Capacity measurement at 1 C-rate; charging with 0.1 C-rate (0.34 A) and discharging with 0.5 C-rate (3.4 A);
6. Repeat steps 0. – 5. for 25°C and 40°C

The current, voltage, and temperature signals, which were logged during the capacity measurement at 10°C are presented in Fig. 2. Each of the above summarized steps of the capacity measurement test are highlighted in Fig. 2.

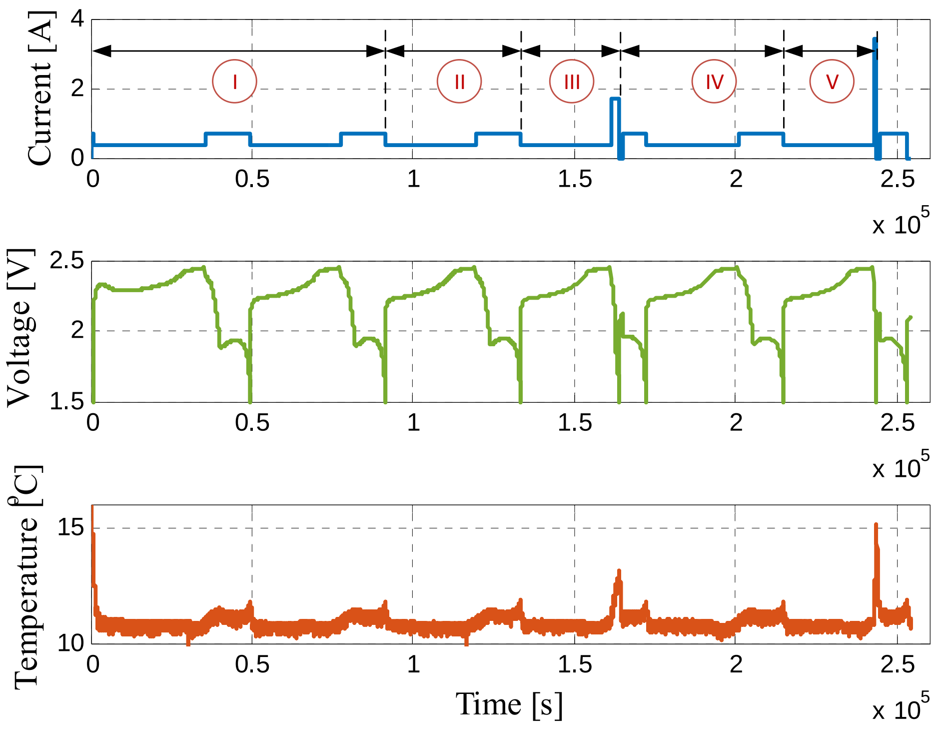

Figure 2. Li-S battery cell current (top), voltage (middle), and temperature (bottom) during the capacity measurement test performed at 10°C.

The preconditioning cycle is applied in order to reset the history of the Li-S battery cell as explained in (12) and to allow for a non-biased comparison of the capacity results at different C-rates.

The dependence of the Li-S battery's capacity on the temperature and C-rate is illustrated in Fig 4; the nine measurement points at which the capacity of the cell was measured are highlighted. As one can observe, the capacity is strongly influenced by the operating temperature. For example, for a C-rate of 1 C-rate, the battery capacity increases by 250%, from 0.968 Ah to 2.534 Ah, for a temperature increase of 30°C (from 10°C to 40°C); nevertheless, for the same temperature range, the capacity increase is less visible at lower C-rates. These results are in good agreement with the results presented in (6) for a similar temperature range and in (13) for a high temperatures range (i.e., 70°C - 90°C).

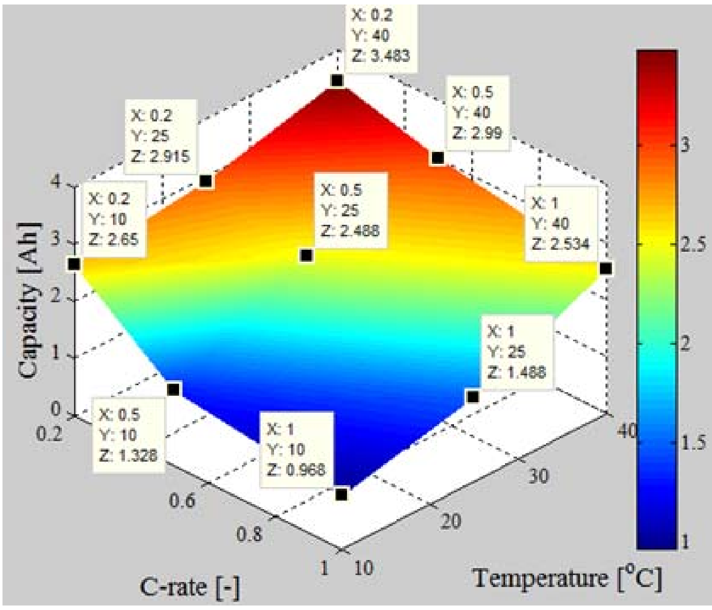

Figure 3. Dependence of the Li-S battery cell's capacity on temperature for different charging rates.

Furthermore, we have investigated the temperature evolution during all the capacity checks, and the results are presented in Fig. 4. We have observed the highest temperature increase during capacity measurement at low temperatures, with a maximum of approximately 4.5°C for the case of 1 C-rate. It is thought that these high temperature deviations at low temperature might have been caused by the increased internal resistance at low temperature which is even more accentuated at the end of the discharge process (i.e., SOC=0%). Moreover, it has to be mentioned that during the discharging process, the temperature of the cell increased monotonously, without any plateaus.

Internal Resistance Measurement

Together with the capacity, the internal resistance is a key battery parameter for battery systems optimal design in any application. This is because the battery internal resistance is closely related to the battery power, which is used for sizing purposes, and developing optimal energy management strategies. Furthermore, the internal resistance is an important parameter for battery cell heat generation modeling – the higher the resistance is, the higher the heat generation in the battery cell will be (11).

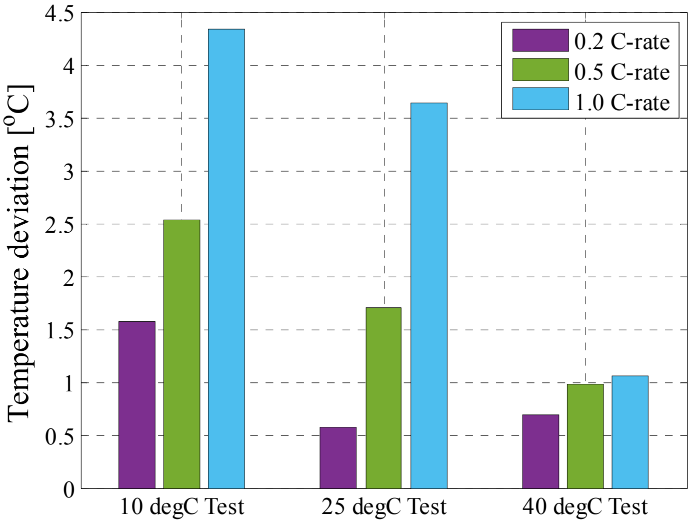

Figure 4. Measured temperature deviation during the capacity tests at different conditions.

The internal resistance of Li-S battery cells is dependent on the temperature and is strongly changing with the SOC (14). Moreover, the internal resistance of the battery cells is increasing, while the cells are ageing; however, this is out of the scope of this work.

Different procedures to measure the battery cells internal resistance can be applied (15); nevertheless, in this work, we have used the traditional DC pulse technique to determine the battery resistance for both charging and discharging conditions. Because, the battery internal resistance is dependent on the load current, we have applied charging and discharging pulses of different amplitudes (i.e., 0.1 C-rate, 0.2 C-rate, 0.5 C-rate and 1 C-rate). The measurements were performed for the 10-90% SOC interval and repeated at 10°C, 25°C, and 40°C.

The Li-S battery cell voltage response to a 20 seconds discharging pulse is presented in Fig. 5. The internal resistance was computed according to Ohm's law as given in [3].

$$Ri = \Delta V / \Delta I = (V1 - V0) / I \qquad [3]$$

Where $V0$ and $V1$ are illustrated in Figure 5 and I is the amplitude of the applied DC pulse.

The variation of the internal resistance with the battery SOC at the three considered temperatures is presented in Fig. 6; these specific values were obtained for a discharging current pulse of 3.4 A. As expected the obtained results show that the internal resistance increases with decrease of temperature. Furthermore, depending on the temperature, the variation of the resistance with the SOC changes its pattern. At 10°C and 25°C, a parabolic dependence on the SOC is observed for the 10% - 70% SOC, which is followed by a step decrease of the internal resistance at SOC higher than 70% SOC. This inflection point, at around 70% SOC, corresponds to the transition from the low voltage plateau to the high voltage plateau. For 25°C and 40°C, the highest resistance was measured at low SOCs, in this case 10% SOC. Additionally, independent on the temperature, the minimum value of the internal resistance is measured at high SOCs; furthermore, as one can observe, the value of the internal resistance at 90% SOC is quasi-independent on the temperature.

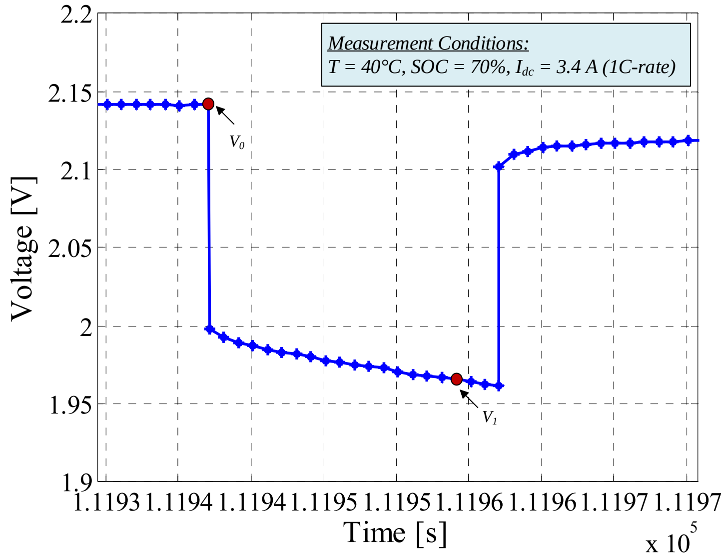

Figure 5. Voltage response of a Li-S battery cell to a discharging current pulse.

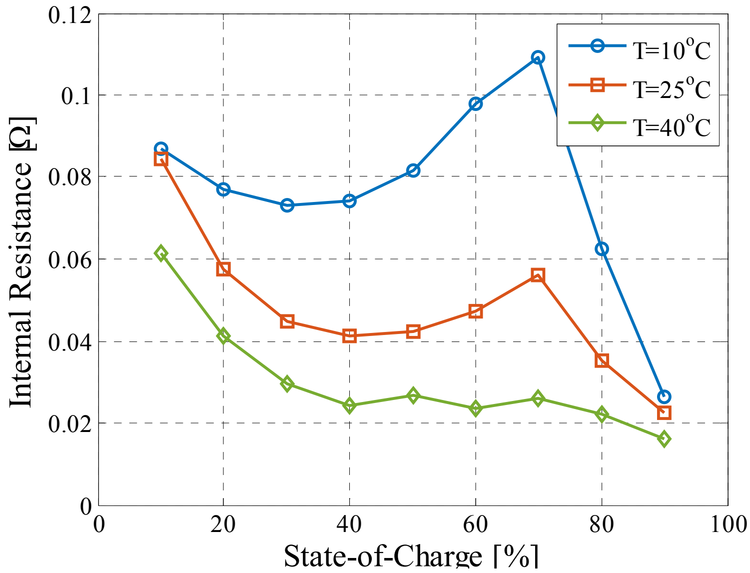

Figure 6. Variation of the internal resistance with the SOC and temperature.

Entropic Heat Coefficient Measurement

The EHC, also referred as temperature coefficient, describes the potential derivative with respect to the temperature and is determined in order to calculate the heat generation within the battery cell. In the literature there are presented several approaches for determining the EHC; however in this work, we have used the open circuit potentiometry technique to determine this coefficient (11). In order to determine the change of the EHC with the SOC, measurements were carried for the SOC interval from 90% to 10%, with a 10% resolution.

Before performing the open circuit potentiometry measurements, a preconditioning cycle was applied to the Li-S battery cell, followed by a full charging process. Then, the cell was discharged to 90% SOC, where it was left at open circuit condition, in order to reach thermo-dynamic stability. Normally, after the SOC was modified, a four hour relaxation period was considered; nevertheless, in order to reduce the influence of the high self-discharge at increased SOC levels (4), the relaxation period at 90% and 80% SOC was reduced to one hour. The relaxation was followed by the thermal cycle illustrated in Fig. 7; each temperature level was maintained for 2 hours, except for the 90% and 80% SOC, where each temperature was applied for one hour, due to the aforementioned limitations.

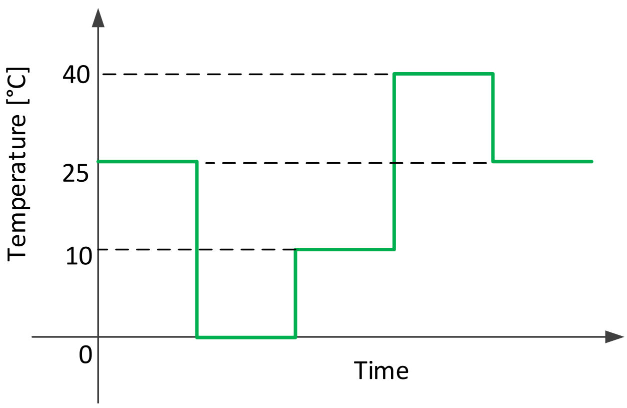

Figure 7. Thermal cycle used to determine the EHC by open circuit potentiometry.

The behavior of the Li-S battery cell voltage during the thermal cycle, at one SOC level, is presented in Fig. 8. The change in the voltage is invers proportional with the change in the temperature, except the temperature increase from 10°C to 40°C, when the battery voltage increases as well. This suggests a negative EHC (11). The same behavior was observed for all the considered SOC levels at which the EHC was measured.

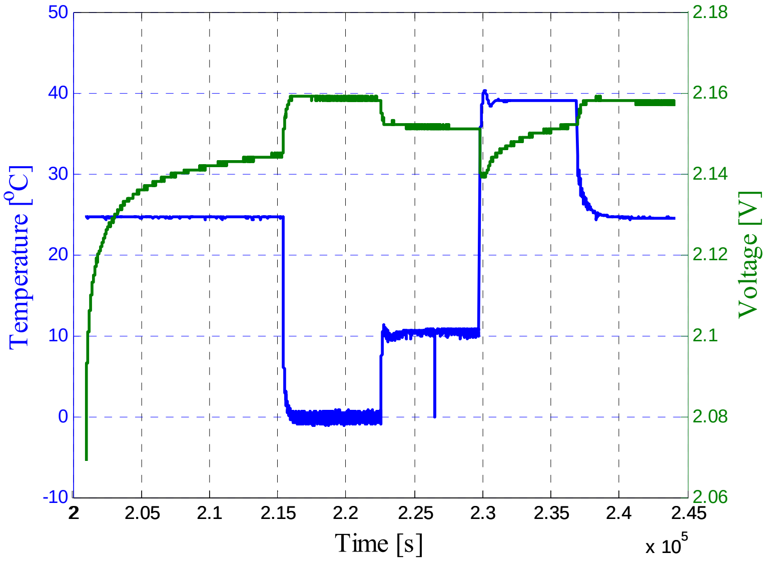

Figure 8. Voltage behavior during the thermal cycle at 50% SOC.

In order to derive the values of the EHC, the voltage profiles obtained at each SOC (as the one presented in Fig. 8), were fitted to the function given in [4] (11). The fitting was carried out using the *Curve Fitting* toolbox from MATLAB®.

$$V(t,T) = A + B \cdot T + C \cdot t \qquad [4]$$

Where, *A*, *B*, and *C* are constants and *B* corresponds to the EHC.

By following this procedure, the values of the EHC at each considered SOC were obtained and are presented in Fig. 9. The EHC has negative values for all the SOC internal, which suggests that the effect of the entropic heat is exothermic during discharging and endothermic during charging, independent on the battery current.

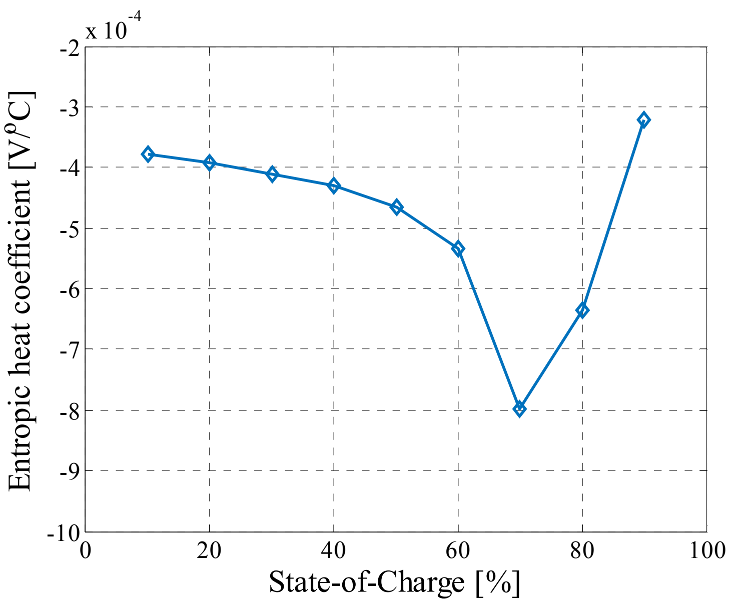

Figure 9. The variation of the EHC as function of SOC.

Conclusions

In this paper we measured the internal resistance and entropic heat coefficient of a 3.4 Ah Li-S battery cell. These are the two parameters necessary to develop a heat generation model, which represents the first step in the development of a battery thermal model. The internal resistance of the battery cell was determined at 10°C, 25°C, and 40°C and it shown a highly nonlinear variation with the SOC. Furthermore, the dependence of the internal resistance on the SOC does not follow the same pattern for all temperatures. The measured EHC has negative values independent on the considered battery SOC suggesting that the effect of the entropic heat is exothermic during discharging (i.e., heat is released) and endothermic during charging (i.e., heat is absorbed).

Acknowledgments

This work has been part of the ACEMU-project. The authors gratefully acknowledge the Danish Council for Strategic Research (1313-00004B) and EUDP (1440-0007) for providing financial support and would like to thank OXIS Energy for supplying the Lithium-Sulfur battery cells.

References

1. P. G. Bruce, L. J. Hardwick, and K. M. Abraham, *MRS Bulletin*, **36**(7), 506-512 (2011).
2. Z. Deng et al., *J. Electrochem. Soc.*, **160**(4), A553 (2013).
3. K. Xie et al., *Adv. Mater.,* **29**, 1604724 (2017).
4. V. Knap et al., *J. Electrochem. Soc.*, **163**(6), A911 (2016).
5. D.-I. Stroe et al., *ECS Trans.,* **72**(12), 13-22 (2016).
6. K. Propp et al., *J. Power Sources* **328**, 289-299 (2016).
7. X. Feng et al., *Phys. Chem. Chem. Phys.*, **16**, 16931 (2014).
8. J. Seo et al., *Electrochemistry Communications*, **44**, 42 (2014).
9. D. Adair et al., *Modern Environmental Science and Engineering*, **2**, 246 (2016).
10. D. Bernardi, E. Pawlikowski, and J. Newman, *J. Electrochem. Soc.*, **132**, 5 (1985).
11. N. Nieto et al., *J. Electrochem. Soc*, **160**(2), A212 (2013).
12. V. Knap et al., *ECS Trans.,* MA2017-01 538 (2017)
13. J, Hassoun and B. Scrosati, *Adv. Mater*., **22**, 5198 (2010).
14. V.S. Kolosnitsyn et al., *J. Power Sources,* **252,** 28 (2014).
15. H.-G. Schweiger et al., *Sensors*, **10**, 5604 (2010).